JOURNAL OF MATERIALS SCIENCE 32 (1997) 5825–5832

Manufacture of biodegradable packaging foams from agar by freeze-drying

JONG-PIL LEE, KUN-HONG LEE*, HYUN-KON SONG
Department of Chemical Engineering, Pohang University of Science and Technology, San 31, Hyoja-Dong, Nam-Ku, Pohang, Kyungbuk, 790-784, South Korea

Cellular foams were made from the aqueous solution of agar by freeze-drying. A narrow range (5–20 °C min^{-1}) of freezing rate was required to avoid damage to the microstructure of the agar foams. The size of cells in the foam decreased with increasing freezing rate. Agar foams of more than 4 wt% agar content absorbed more energy than a polystyrene foam in compression tests. Foams with a higher agar content absorbed more energy. The behaviour of agar foams in compression tests could be explained by the modified beam theory for cellular foams. Agar foams were thermally stable up to 200 °C, and were also stable in a humid environment.

Nomenclature

E_s	Young's modulus of solid agar
E^*	Young's modulus of an agar foam
p_{at}	atmospheric pressure
p_0	initial pressure of gas inside the cells of an agar foam
ε	strain
$\dot{\varepsilon}$	strain rate
ε_D	full densification strain
ϕ	solid fraction contained in the cell edges
ν^*	Poisson's ratio
ρ^*	apparent density of an agar foam
ρ_s	density of solid agar
σ	stress
σ^*	plateau stress
σ^*_{el}	elastic collapse stress
σ_p	maximum permitted packaging stress

1. Introduction

Polystyrene foams are commonly used as packaging materials and insulators. About 70 000s ton of polystyrene foams were used as packaging materials in South Korea in 1993. However, the biological and chemical stability of polystyrene foams can cause environmental problems unless they are recycled in a proper way. Moreover, the typical blowing agents used in making polystyrene foams include halocarbons [1] which are of concern both for their ozone depletion potential and for their impact on global warming. Various attempts have been made worldwide to enhance the biodegradability of packaging foams or to substitute blowing agents which are environmentally friendly for the halocarbons.

Biodegradable foams can be made without using blowing agent. A new family of lightweight foams were recently synthesized from an aqueous solution of agarose [2, 3]. These foams are completely biodegradable (even edible), and may make a good replacement for packaging foams, insulation for refrigerators, and capsules for time-release drugs. Agarose foams were reported to be as strong as balsawood with half the density [4].

In this study, biodegradable foams for use as packaging materials were manufactured from an aqueous solution of agar by freeze-drying. The effects of process conditions, such as concentrations of agar, freezing rates and temperatures on the physical properties and microstructures of the agar foams were investigated. Modified beam theory for cellular foams was applied to specify the characteristics of agar foams.

2. Experimental procedure

The experimental procedure to prepare agar foams consists in three steps as shown in Fig. 1, gelation, freezing and vacuum drying.

Agar powder (Junsei Chemical Co.) was used as-received. Fourier transform–infrared (FT–IR; Mattson Co., Polaris™) measurements were performed to identify the components of the agar powder used in this study. FT–IR spectra were obtained using films prepared by evaporation of an aqueous solution of agar in an oven at 80 °C for 10 h.

1, 2, 4 and 8 wt% aqueous solutions of agar were prepared by dissolving agar powder in distilled water at 90 °C. These solutions were poured into disc-shape

*Author to whom correspondence should be addressed.

0022–2461

moulds (3.3 cm diameter and 1.0 cm high) and left at room temperature for 24 h for gelation.

Four different freezing methods were used at the freezing step. Samples were identified by a letter for the different freezing methods, and a number indicating the weight per cent of agar. For example, sample V4 was prepared by using cold nitrogen gas for freezing, and its agar content was 4 wt%. Samples C were prepared by placing an agar gel in the cold chamber of 252.1 K for 24 h. Samples V were prepared under flowing cold nitrogen gas for 20 min evaporated from liquid nitrogen. Samples I were prepared by immersing agar gels into liquid nitrogen for 1 min.

All the frozen gels were placed in the vacuum apparatus shown in Fig. 2 for vacuum drying. Water vapour sublimated from frozen gels is continuously removed by a rotary vacuum pump (Sargent-Welch Scientific Co., 8851C). Water vapour is frozen on the wall of the liquid nitrogen trap, which prevents contamination of the rotary vacuum pump and maintains a high vacuum in the sample flasks. The pressure inside the sample flasks is detected by the convectron vacuum gauge (Granville-Phillips Co., Series 275). The vacuum inside the apparatus was controlled by valves. The temperatures of the samples during drying were measured by using a thermocouple inserted into the samples. The base vacuum was 20 mtorr (1 torr = 133.322 Pa) and the operating condition was in the range of 100–300 mtorr. Agar foams were prepared after 30 h vacuum drying to guarantee complete drying. In addition to the above mentioned samples, S foams were prepared by a self-freezing method. An agar gel at room temperature was vacuum dried without pre-freezing.

The microstructures of agar foams were investigated by scanning electron microscopy (Cambridge Instruments, Stereoscan 250 MK3; Jeol, JSM-840A; and Phillips, SEM515). True densities of agar were measured using a helium pycnometer (Quantachrome Co., Multipycnometry) while the apparent bulk densities of agar foams were calculated from the measured dimensions and weights of agar foam samples. The compressive strength of agar foams was measured using the Universal Testing Machine (Instron, Model 4206). Thermal analysis was also carried out with the thermogravimetric analyser (Perkin Elmer, TGA2) and the differential scanning calorimeter (Perkin Elmer, DSC7). The heating rate was 10 °C in TGA, and two runs were made in DSC measurements for each sample to eliminate any moisture effect. The heating rates of the first and second runs were 20 and 10 °C min^{-1} respectively. For the investigation of the moisture sensitivity of agar foams, samples were placed in a constant temperature, constant humidity chamber at 25° and 96% relative humidity. The weights of samples were measured for 13 days at 24 h intervals.

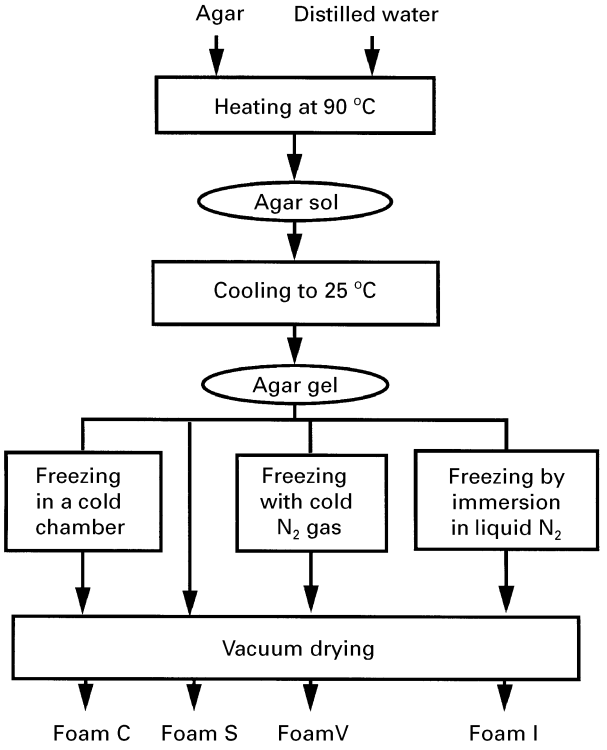

Figure 1 Manufacturing process of agar foams.

3. Results and discussion

3.1. Characterization of agar

Fig. 3 shows the FT–IR data of an agar sample prepared by the method mentioned in the previous

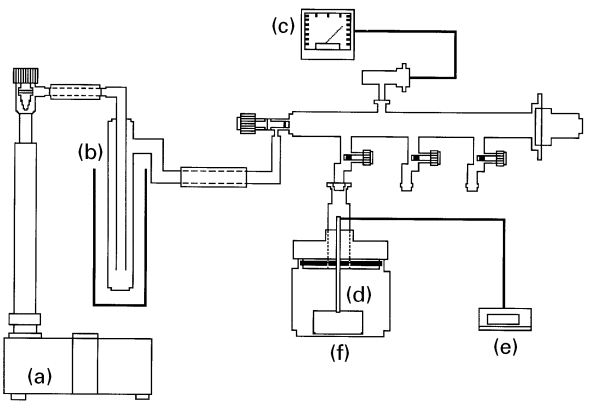

Figure 2 Schematic diagram of the vacuum drying apparatus. (a) Vacuum pump, (b) liquid nitrogen trap, (c) vacuum gauge, (d) thermocouple, (e) temperature indicator, (f) sample holder.

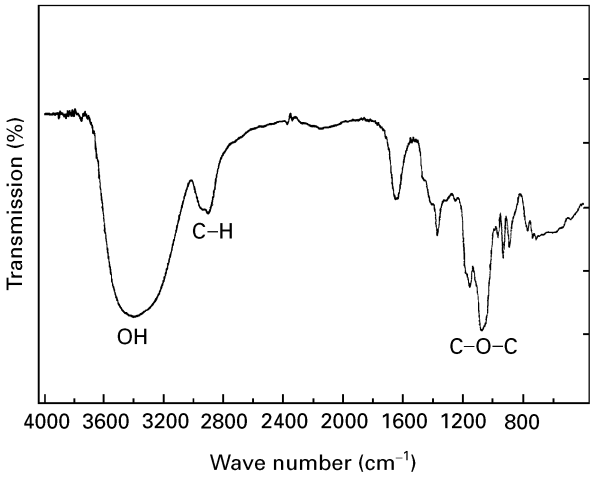

Figure 3 FT–IR spectrum of agar used in this study.

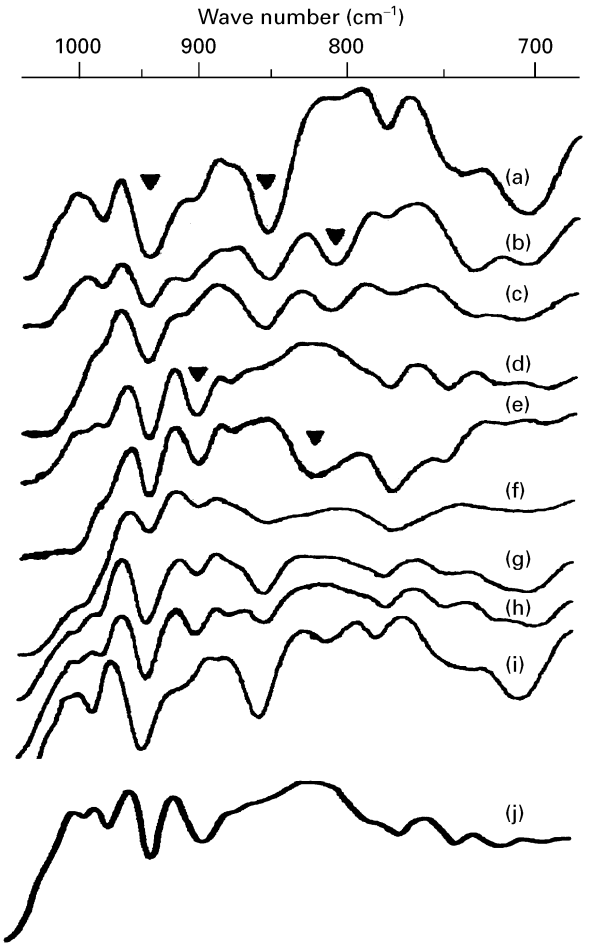

Figure 4 FT–IR spectra of polysaccharides from (a) *Eucheuma cottonii*, (b) *Eucheuma spinosum*, (c) *Sarcodiotheca furcata*, (d) *Gelidium amansii*, (e) *Gloiopeltis furcata*, (f) *Odonthalia kamtschatica*, (g) *Furcellaria fastigiata*, (h) *Endocladia muricata*, (i) the KCl-insoluble fraction from *Chondrus crispus* [5], and (j) agar used in this study.

section. The wide bands at 3200–3600, 2800–3000, and 1000–1200 cm^{-1} are due to O–H stretching, C–H stretching and C–O–C stretching, respectively. The FT–IR spectra of various polysaccharides are shown in Fig. 4 [5]. Also included in this figure is the FT–IR spectrum of Fig. 3 in the frequency range 700–1000 cm^{-1}. The FT–IR spectrum of the agar sample prepared in this study is similar to that of *Gelidium amansii* (Fig. 3d). The intense band at 940 cm^{-1} is due to 3,6-anhydrogalactose residues and the band at 895–900 cm^{-1} is a characteristic of *Gelidium amansi.*

3.2. Freezing rate

Four different freezing methods were investigated in this study. The main difference between these methods was the freezing rate. Agar foams indicated by C, S, V and I were prepared at freezing rates of ca. 0.6, 7, 15 and 220 °C min^{-1}, respectively, followed by vacuum drying. Fig. 5 shows agar foams which were manufactured from 2 wt% aqueous solution of agar. Foam C2 reduced in size during vacuum drying, and ended with a transparent foam with rough surfaces. On the contrary, no significant damage to the structure was found in foams S2 and V2. They remained unchanged during vacuum drying, and ended as translucent foams. They were almost identical in shape, size and surface roughness. Foam I2 was destroyed during immersion freezing due to the thermal shock of rapid cooling. Violent boiling of liquid nitrogen and thermal shock resulted in the contraction of the outer surface of agar gels, and the gel cracked. However, no crack occurred with foams S2 and V2, as shown in Fig. 5. The reduction of thermal shock prevented them from cracking and peeling. Therefore, the freezing rate is an important operating variable to obtain undamaged agar foams. The optimum freezing rate was in the range 5–20 °C min^{-1} for the samples considered in this study.

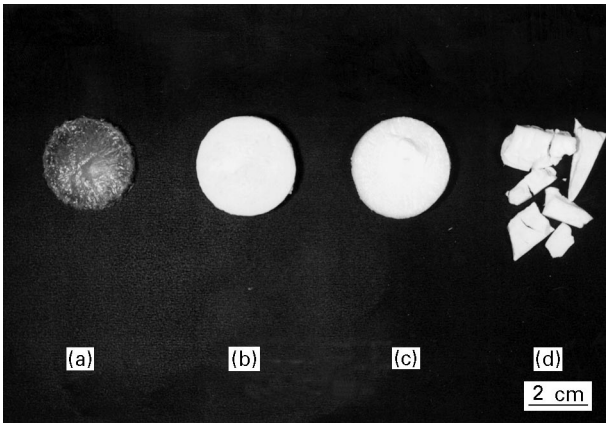

Figure 5 Effect of freezing rate on the shape of agar foams. (a) Foam C2, (b) foam S2, (c) foam V2, (d) foam I2.

The effect of freezing rate on the microstructures of agar foams is clearly demonstrated in Fig. 6. Large pores resulted from the formation of large ice crystals due to the slow freezing rate as shown in the foam C2. In contrast, relatively small pores were found in foam S2. A sheet structure was found in both samples, so they formed closed cells that could withstand external forces, thus explaining the elastomeric foam-like characteristics of agar foams when they were compressed. On the other hand, both closed cells and open cells were found in the foam V2, suggesting that freezing with cold nitrogen gas was at a greater freezing rate. It is expected that the portion of open pores increases with the freezing rate; thus is quite obvious from the scanning electron micrograph of foam I2, in which virtually no closed cells were found.

3.3. Density of agar foams

Fig. 7 shows the measured bulk densities of agar foams versus target densities. The target density is the density of the agar foams when there is no contraction of the agar gels during freezing and vacuum drying. The difference between target densities and measured densities increases with the amount of agar in the starting aqueous solution of agar. Foams C always resulted in higher bulk densities than other samples, proving that the formation of large ice crystals caused some breakage of the gel network, and therefore the contraction of volume occurred due to the stress exerted during vacuum drying.

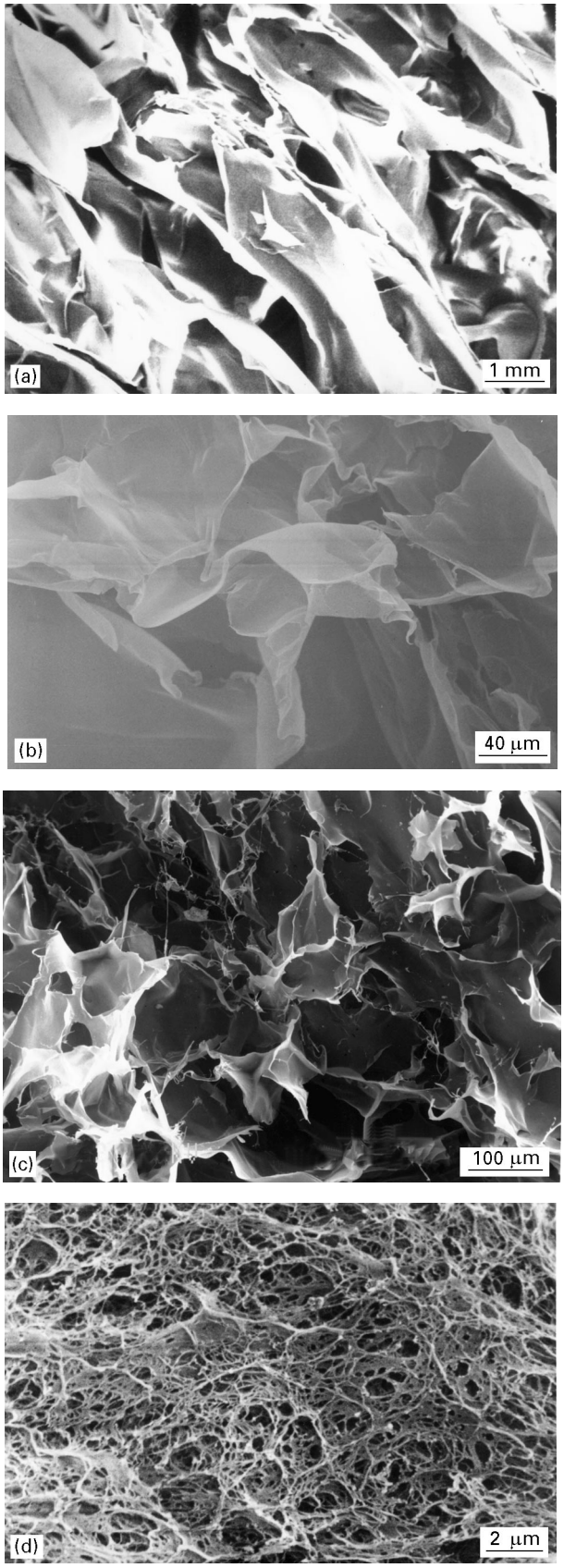

Figure 6 Effect of freezing rate on the microstructure of agar foams. (a) foam C2, (b) foam S2, (c) foam V2, (d) foam I2.

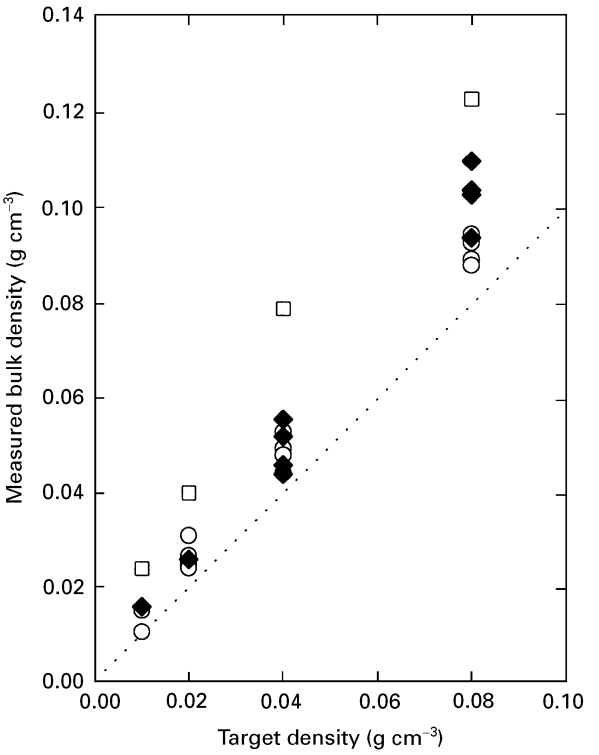

Figure 7 Shrinkage of agar foams during freeze-drying, (□) foam C, (◆) foam V, (○) foam S.

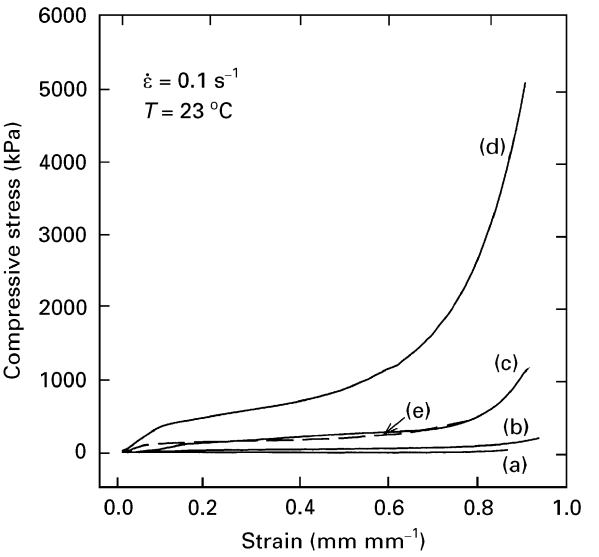

Figure 8 Compressive stress–strain curves for foams S and a polystyrene foam. (a) Foam S1, (b) foam S2, (c) foam S4, (d) foam S8, (e) polystyrene foam ($\dot{\varepsilon} = 4 \times 10^{-3}\ s^{-1}$, $\rho^*/\rho_s = 0.1$).

3.4. Compressive strength

Most applications of foams cause them to be loaded in compression. Figs 8 and 9 show the compressive stress–strain curves for foams S and V, respectively. The curve of a polystyrene foam used for a microcomputer package also appears for comparison. All of these graphs exhibit typical characteristics of elastomeric foams. They show linear elasticity at low stress, followed by a long collapse plateau, truncated by a regime of densification in which the stress rises steeply. It is clearly shown that modulus and plateau stress increase as the content of agar increases. The relative thickness of the cell walls increases with the content of agar, resulting in greater resistance to wall bending and cell collapse during the compression test [6]. Foams V4, V8, S4 and S8 presented better performances in energy absorption than the polystyrene foam considered here.

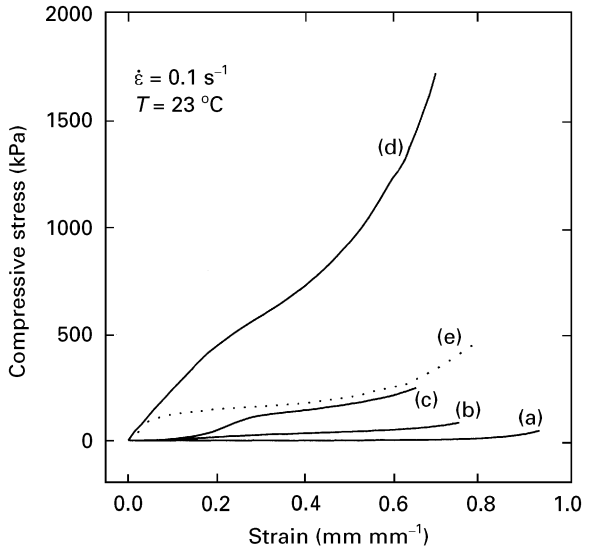

Figure 9 Compressive stress–strain curves for foams V and a polystyrene foam. (a) Foam V1, (b) foam V2, (c) foam V4, (d) foam V8, (e) polystyrene foam ($\dot{\varepsilon} = 4 \times 10^{-3}$ s^{-1}, $\rho^*/\rho_s = 0.1$).

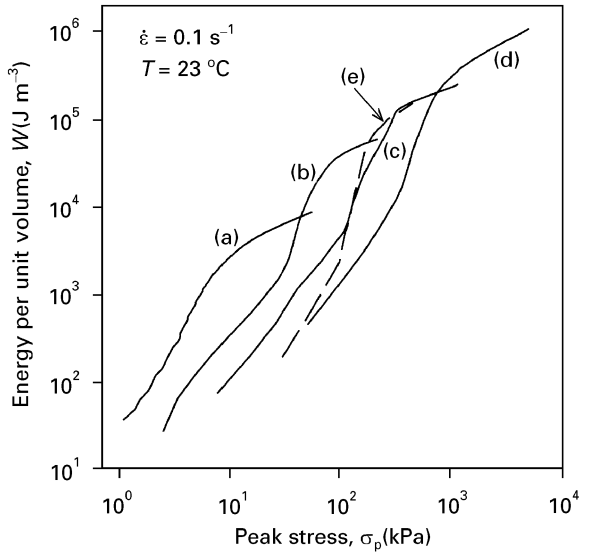

Figure 10 Energy absorption curves for foams S and a polystyrene foam. (a) Foam S1, (b) foam S2, (c) foam S4, (d) foam S8, (e) polystyrene foam ($\dot{\varepsilon} = 4 \times 10^{-3}$ s^{-1}, $\rho^*/\rho_s = 0.1$).

The energy-absorption diagrams shown in Figs 10 and 11 were generated from the integration of the area occupied by the compressive stress–strain curves. The energy-absorption diagram is necessary for the optimum choice of foams. The best foam for a given package is one that absorbs the most energy up to the maximum permitted packaging stress, σ_p. Optimum σ_p is determined by the shoulder on the energy–absorption curve of a foam. The peak stress of the polystyrene foam was 410 kPa. Foams V4, V8, S4 and S8 presented better performance in energy absorption than the polystyrene foam. It is obvious in these figures that more energy can be absorbed with higher density foams.

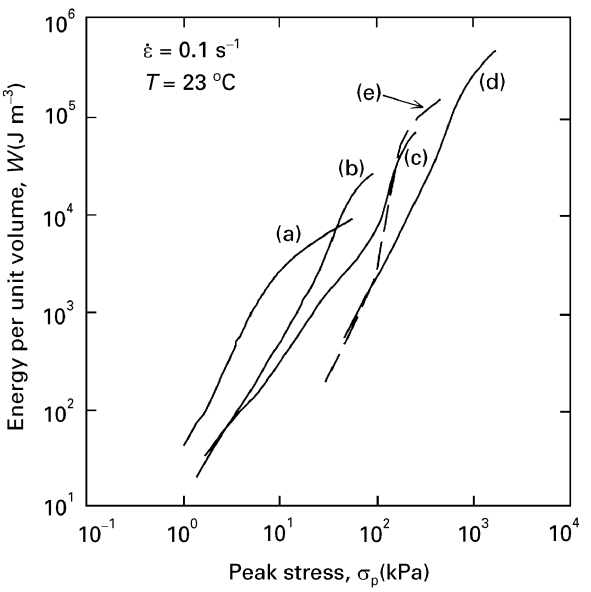

Figure 11 Energy absorption curves for foams V and a polystyrene foam. (a) Foam V1, (b) foam V2, (c) foam V4, (d) foam V8, (e) polystyrene foam ($\dot{\varepsilon} = 4 \times 10^{-3}$ s^{-1}, $\rho^*/\rho_s = 0.1$).

3.5. Mechanics of agar foams

Modified beam theory for cellular foams [6] was used to analyse the response of agar foams to the compression test. The elastomeric behaviour of a cellular foam strongly depends on the shape of cells in the foam. Foams S consist of closed cells as clearly shown in Fig. 7b, so the theory developed for closed cells was used to analyse the elastomeric behaviour of S foams. In addition to the bending of cell walls, the pressure of gas enclosed inside the cells and membrane stretching have effects on the mechanics of cell deformation.

The densification of foams S is shown in Fig. 12. Full densification strains, ε_D, of foams S with different agar contents were plotted together with the experimental correlation of Maiti *et al.* [7]. The agreement between the full densification strains of foams S and the correlation was very good, even though this correlation was developed for the foams of synthetic polymers.

The plateau stress, σ^*, plotted against the remaining gas volume, $\varepsilon/(1 - \varepsilon - \rho^*/\rho_s)$, for foams S is shown in Fig. 13. Plateau stresses of foams S rise with increasing strain. This behaviour is ascribed to the compression of the gas enclosed in the closed cells of foams S as the cells collapse, creating a restoring pressure. A semi-theoretical equation for the plateau stress of closed-cell foams in the post-collapse region is [6]

$$\sigma^* = \sigma^*_{el} + \frac{p_0 \varepsilon}{1 - \varepsilon - \rho^*/\rho_s} \quad (1)$$

If we accept the above equation, the elastic collapse stress, σ^*_{el}, and initial gas pressure, p_0, can be easily obtained from, respectively, the intercept and the slope of data shown in Fig. 13. The slopes of data for foams S, however, increase with density even though the theory is established on the assumption of constant initial gas pressure. It is known that the gas

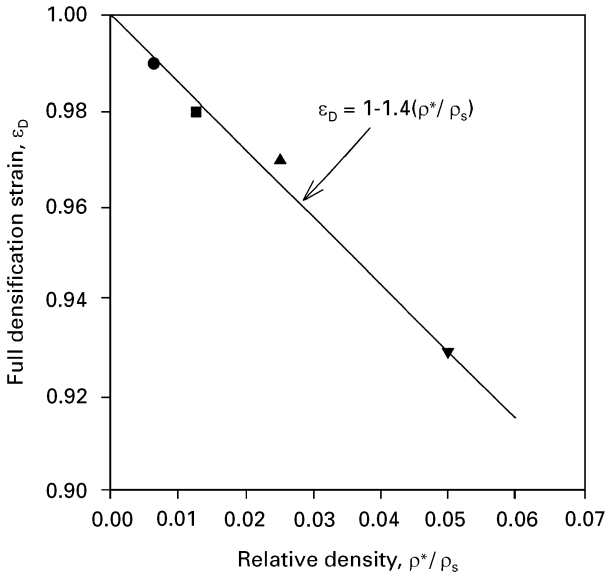

Figure 12 Full densification strain of foams S in the densification region: (●) S1, (■) S2, (▲) S4, (▼) S8.

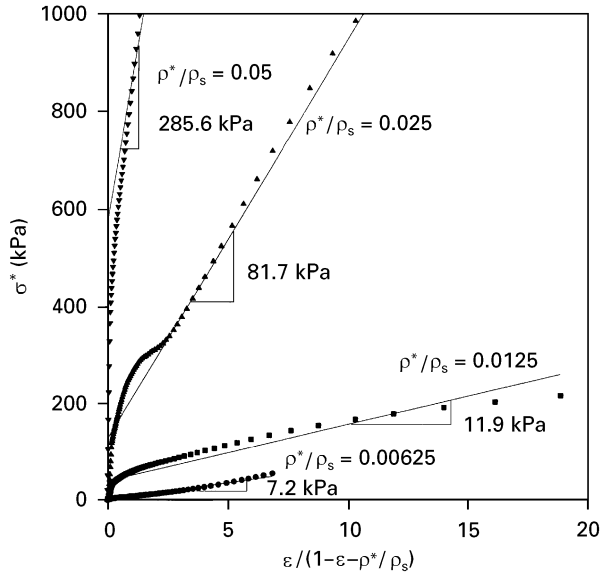

Figure 13 Plateau stress of foams S in the post-collapse region: (●) S1, (■) S2, (▲) S4, (▼) S8.

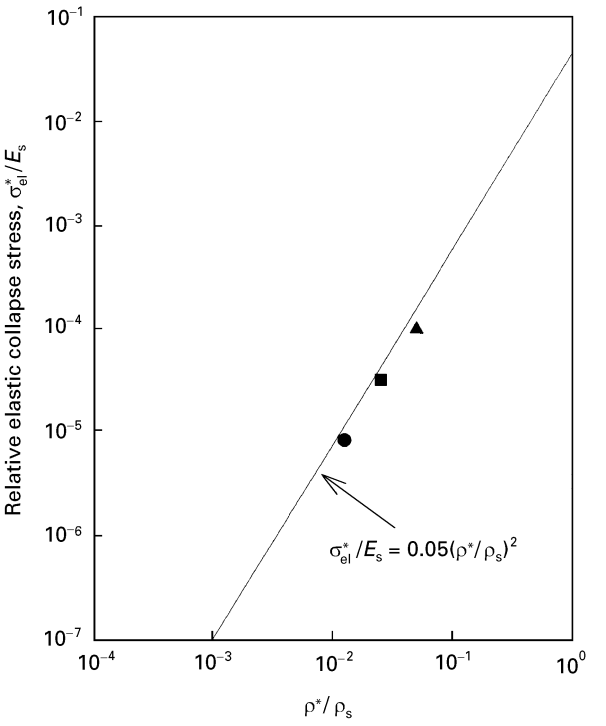

Figure 14 Normalized elastic collapse stress of foams S: (●) S2, (■) S4, (▲) S8.

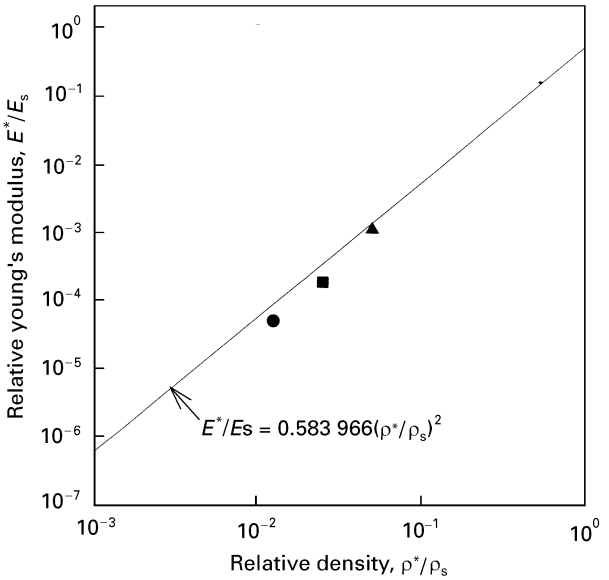

Figure 15 Relative Young's modulus of foams S: (●) S2, (■) S4, (▲) S8.

compression is the dominant contribution to the rising plateau in low-density foams [8], but the membrane stress becomes more important in the high-density foams which have more material in cell faces. The trend seen in Fig. 13 is in accordance with the foams made with synthetic polymers [7].

The stress at the initiation of collapse (elastic collapse stress), σ^*_{el}, is better understood from theory. Fig. 14 shows the relative elastic collapse stress, σ^*_{el}/E_s, of foams S, together with a semi-theoretical equation for closed-cell foams. To construct this figure, σ^*_{el} was obtained from the intercepts of Fig. 13, and the Young's modulus of solid agar (not foams), E_s, was assumed to be 3560 MPa. The gas-pressure contribution is neglected in the equation, because the gas pressure inside the cells of a foam is about the same order as atmospheric pressure in artificial foams, so the term with $(p_0 - p_{at})$ is small compared with the other term.

Relative Young's moduli, E^*/E_s of foams S are plotted in Fig. 15 as a function of relative density, ρ^*/ρ_s. Also shown in this figure is the theoretical expression fitted to the experimental data.

$$\frac{E^*}{E_s} \approx \phi^2 \left(\frac{\rho^*}{\rho_s}\right)^2 + (1-\phi)\frac{\rho^*}{\rho_s} + \frac{p_0(1-2\nu^*)}{E_s(1-\rho^*/\rho_s)}. \quad (2)$$

Equation includes the contributions of membrane stresses and the pressure of gas enclosed in the cells. Because the second and the third terms, however, were small compared with the first term, a simplified

equation was used in the fitting of experimental data. The solid material in the cell face can be calculated from the slope of data in Fig. 15. About 24% of the total agar content of foams S was retained in the cell face.

3.6. Thermal stability

Fig. 16 shows the result of thermogravimetric analysis for the foam I1. The first weight loss between 80 and 120 °C is attributed to the evaporation of surface water. A major weight loss began around 300 °C and the weight reached about 25% of the initial weight in the proximity of 360 °C. The TGA curves of agar foams with different freezing methods were alike.

The DSC curve of the foam S1 is shown in Fig. 17. This curve confirms the results of TGA data. Agar foams with different freezing methods were alike. Fig. 18 shows the volume change upon heating. Foams S4 do not change at all up to 190 °C while polystyrene foam shrinks noticeably in the samples treated at 170 and 190 °C.

3.7. Moisture stability

Resistance to moisture is a required property of a packaging material. Fig. 19 shows the change in weight of agar foams in a humid environment. About 30% increase in weight was observed in all agar foams after 1 day, followed by a small fluctuation in weight thereafter. All agar foams showed a similar weight increase, regardless of the freezing method. Therefore, agar foams can be used as packaging foam, even in a humid environment, provided there is no direct contact with water.

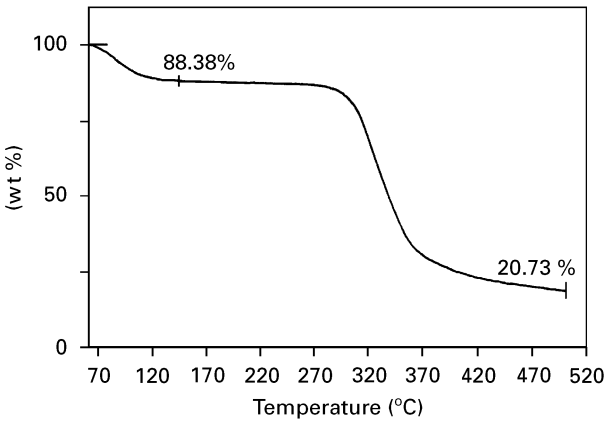

Figure 16 TGA data of the foam I1.

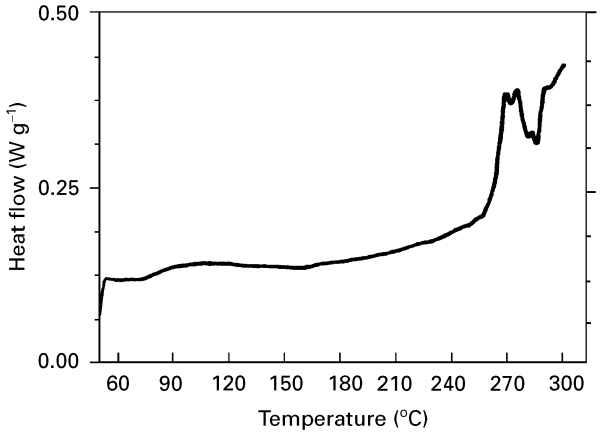

Figure 17 DSC data of the foam S1.

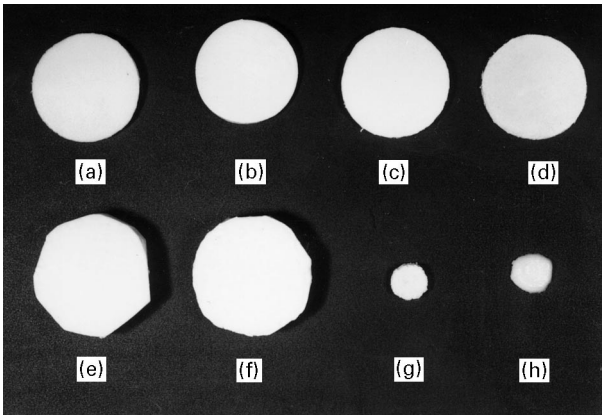

Figure 18 Thermal stability of the foam S4 and a polystyrene foam. (a–d) foam S4, (e–h) polystyrene foam, (a, e) 25 °C, (b, f) 90 °C, (c, g) 170 °C, (d, h) 190 °C.

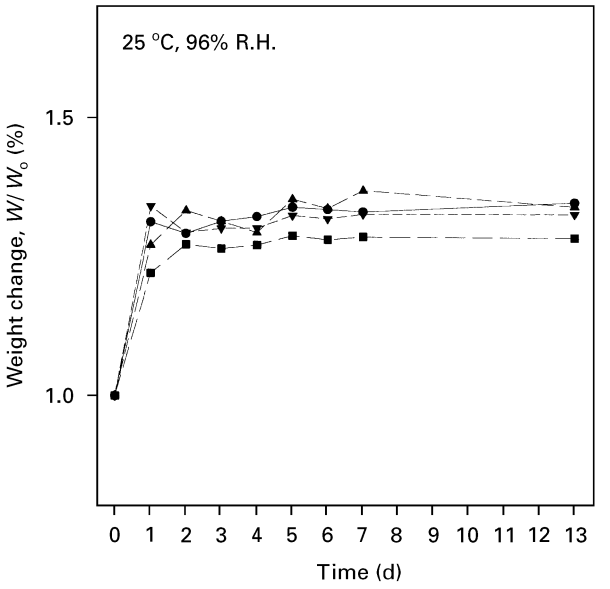

Figure 19 Moisture stability of the foams: (●) S2, (■) I2, (▲) C2, (▼) V2.

4. Conclusions

Biodegradable foams were made from aqueous solutions of agar by freeze-drying. These agar foams possessed many favourable properties as packaging foams; high energy absorption, thermal stability, moisture stability and complete biodegradability.

The morphology and the size of cells were affected by the freezing rate of the agar gels. The amount of energy absorbed in the compression test

was a strong function of the agar content of the foams.

The behaviour of agar foams in the compression test was well described by the modified beam theory for cellular foams. Semi-theoretical equations, developed for the synthetic foams of polymers, were equally applicable to agar foams.

In addition to the complete biodegradability, thermal stability and moisture stability of agar foams ensure future applications in various fields.

Acknowledgements

The authors acknowledge partial support of this work under grants from the Automation Research Center and the Pohang Iron and Steel Company.

References

1. K. W. SUH and R. E. SKOCHDOLPOLE, Foamed Plastics, in the "Kirk-Othmer Encyclopedia of Chemical Technology", 3rd Edn, Vol. 11 (Wiley, New York, 1980) p. 82.
2. R. L. MORRISON, US Pat. 5382 285 (1995).
3. *Idem*, US Pat. 5360 828 (1994).
4. A. CHAIKIN, *Pop. Sci.* February (1993) 72.
5. J. N. C. WHYTE, S. P. C. HOSFORD and J. R. ENGLAR, *Carbohydr. Res.* **140** (1985) 336.
6. L. J. GIBSON and M. F. ASHBY, "Cellular Solids" (Pergamon, 1988).
7. S. K. MAITI, L. J. GIBSON and M. F. ASHBY, *Acta Metal.* **32** (1984) 1963.
8. J. ZHANG and M. F. ASHBY, "CPGS Thesis" (Cambridge, UK 1988).

Received 13 November 1995
and accepted 7 January 1996